

## Calibrating thermal and scanning tunnelling microscope induced desorption and diffusion for the chemisorbed chlorobenzene/Si(111)7 × 7 system

This article has been downloaded from IOPscience. Please scroll down to see the full text article.

2010 J. Phys.: Condens. Matter 22 084002

(<http://iopscience.iop.org/0953-8984/22/8/084002>)

View [the table of contents for this issue](#), or go to the [journal homepage](#) for more

Download details:

IP Address: 129.252.86.83

The article was downloaded on 30/05/2010 at 07:13

Please note that [terms and conditions apply](#).

# Calibrating thermal and scanning tunnelling microscope induced desorption and diffusion for the chemisorbed chlorobenzene/Si(111)-7 × 7 system

S Sakulsermsuk, P A Sloan<sup>1</sup>, W Theis and R E Palmer

Nanoscale Physics Research Laboratory, University of Birmingham,  
Birmingham B15 2TT, UK

E-mail: [p.a.sloan@bham.ac.uk](mailto:p.a.sloan@bham.ac.uk)

Received 24 August 2009, in final form 5 October 2009

Published 4 February 2010

Online at [stacks.iop.org/JPhysCM/22/084002](http://stacks.iop.org/JPhysCM/22/084002)

## Abstract

The precise calibration of thermally driven processes in scanning tunnelling microscope (STM) manipulation experiments, especially at room temperature and above, is necessary to uncover an accurate picture of non-thermal dynamical processes such as desorption induced by electronic transitions, driven by the STM current. Here we probe the displacement (the sum of desorption and diffusion) of chlorobenzene molecules chemisorbed on the Si(111)-7 × 7 surface, induced both by the STM electrical current and by heat. We also establish truly passive imaging inspection parameters. The activation energy for pure thermal displacement is  $580 \pm 20$  meV, possibly associated with excitation to a physisorbed precursor state. STM induced displacement shows a marked decrease with increasing temperature, once the thermal effects are removed.

## 1. Introduction

The scanning tunnelling microscope makes it possible to initiate dynamical surface processes on a local basis. Processes induced by the STM are non-thermal in nature, for example, the mechanical movement of atoms on a surface [1], direct vibrational [2] or rotation [3] excitation of molecules by tunnelling electrons, electric field effects causing adsorbate movement [4], or electronic excitations caused by the tunnelling electrons [5]. This last category falls into the regime of desorption induced by electronic transitions (DIET) processes [6–14] and may be mediated by electronic capture into negative ion resonance states [15–17]. Such electronic excitation can lead to a range of outcomes including bond-breaking [18] and (intact) molecular desorption [10]. One system that manifests both these channels when excited by the tunnelling current from an STM tip is chemisorbed chlorobenzene on the Si(111)-7 × 7 surface [19–23].

The key to the (one electron) STM desorption of chlorobenzene from the Si(111)-7 × 7 surface is the unsaturated

nature of the adsorbate, which results in low lying empty (and filled) electronic states which are therefore accessible to the tunnelling electrons (or holes) [24–26]. The STM induced C–Cl dissociation proceeds via a more complex process that requires two electrons [23]. In our previous work we considered a possible C–Cl dissociation mechanism in which the first electron induces vibrational excitation of the C–Cl out-of-plane wag mode, which mixes the C–Cl  $\sigma^*$  and low lying  $\pi^*$  orbitals of the molecule, and the second electron attaches to the still vibrationally excited molecule and initiates dissociative electron attachment (DEA) [27, 28]. A test of this (thermally assisted STM) mechanism would be to heat the surface and excite the wag mode ( $\sim 60$  meV) thermally, such that only a single electron is required for dissociation. Such an investigation would require us to calibrate the response of the system to ‘pure’ heating. Thus we present here the thermal dependence of STM induced displacements, desorption and diffusion, for chemisorbed chlorobenzene on the Si(111)-7 × 7 surface. We find that the probability per injected electron of causing such a molecular ‘displacement’ event decreases as the temperature is increased, once pure thermal effects are properly accounted for.

<sup>1</sup> Author to whom any correspondence should be addressed.

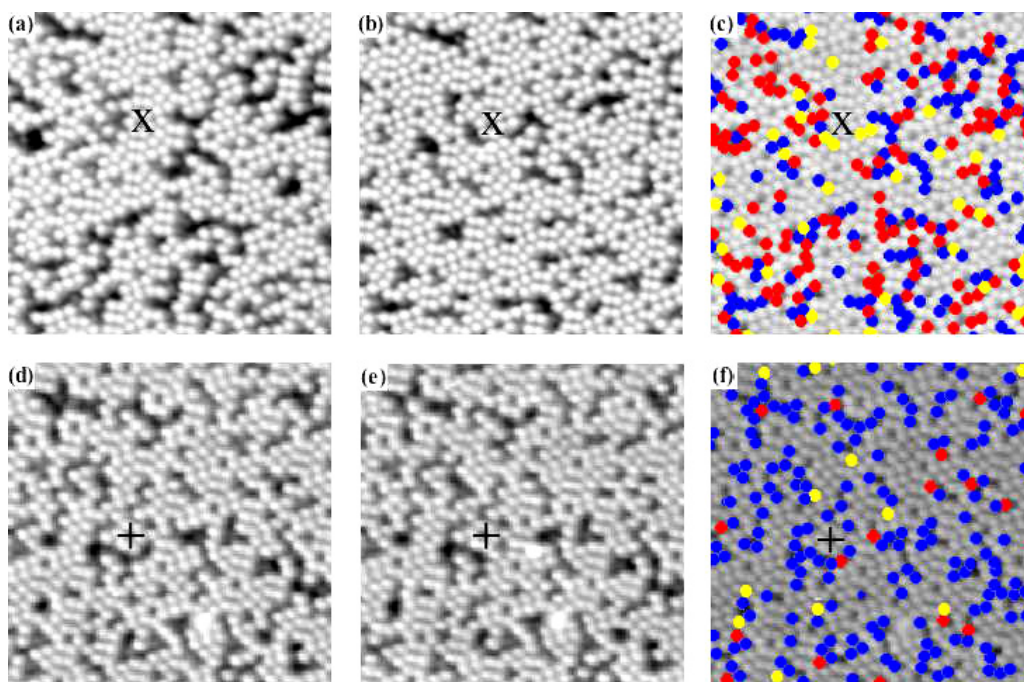


**Figure 1.** STM induced and thermally induced displacement of chlorobenzene molecules on Si(111)-7 × 7. (a) and (b) STM images taken with passive imaging parameters (+1 V, 100 pA, 200 Å × 200 Å) before and after an STM image taken with parameters (+3 V, 50 pA) that induce molecular displacement at  $33.5 \pm 1$  °C. The time lapse between (a) and (b) was 237 s. (c) Computer analysis indicating the locations of sites with molecules before and after (blue/black circles), sites with molecules only before (red/grey) and sites with molecules only after the manipulation scan (yellow/white). ‘X’ marks the same location in panels ((a)–(c)) for reference. (d) and (e) STM images taken 242 s apart with passive imaging parameters (+1 V, 100 pA, 200 Å × 200 Å) at  $30.5 \pm 1$  °C to investigate purely thermal effects. (f) Computer analysis of (d) and (e). The ‘+’ sign marks the same location in panels ((d)–(f)) for reference.

(This figure is in colour only in the electronic version)

## 2. Experimental details

The experiments were performed with an RHK 400 STM in an ultra-high vacuum chamber with a base pressure of  $6 \times 10^{-11}$  Torr. Radiative heating was used to heat the sample to temperatures above room temperature. Tungsten tips were etched by the drop-off technique. The anode electrode was a circular gold wire. A bias of 9 V and a 2 M concentration of NaOH were employed. Etched tips were washed in distilled water. To remove tungsten oxide the tips were resistively heated in a high vacuum chamber [29]. Silicon samples were cut from phosphorous-doped n-type (1–30 Ω cm) wafers of Si(111). These were degassed at  $\sim 600$  °C in the UHV chamber for a few hours, before being resistively flashed, typically for 10 s, to increasing temperatures up to 1250 °C. The sample temperature was measured using a pyrometer (emissivity of silicon of 0.65).

## 3. Results and discussion

To probe the thermal and STM induced molecular desorption and diffusion two similar experimental procedures were followed. Figure 1 shows two ‘passive’ +1 V STM images taken (a) before and (b) after an image that was taken with tunnelling parameters of +3 V and 50 pA that induced molecular displacement. Chlorobenzene forms a 2,5 di- $\sigma$  bonded structure on the Si(111)-7 × 7 surface where two carbon

atoms on opposite sides of the benzene ring form bonds to an adatom and restatom pair [30]. Due to their dangling bond, silicon adatoms image as bright protrusions in unfilled (+1 V) STM images, upon bonding to a chlorobenzene adsorbate the dangling bond is lost and hence the adatoms bound to an adsorbate molecule image as dark ‘missing’ adatom-like features. The signature of a chlorobenzene adsorbate is therefore the darkening of a silicon adatom site. Just by eye the reduction in the number of molecules (dark spots) from figures 1(a) to (b) is apparent. Similarly, figures 1(d) and (e) are passive +1 V STM images taken before and after a specified time lapse to allow pure thermally induced molecular displacement. To calculate the probability per electron, or the thermally induced rate, an in-house written computer program was used to compare the molecules in pairs of passive ‘before’ and ‘after’ images, e.g., (a) with (b), and (d) with (e) in figure 1.

When seeking to compare two STM images directly, e.g., by image subtraction or auto-correlation, there are problems associated with thermal drift and piezo-creep. Images that are aligned at their centres may well be misaligned towards their edges. On the Si(111)-7 × 7 surface any misalignment greater than  $\sim 5$  Å will result in an incorrect comparison of sites in the ‘before’ and ‘after’ images. Misalignment problems are especially pronounced when imaging at elevated temperatures. Here we use a method that probes the unit cells of each image and removes such problems from our analysis. The program initially determines the position of each unit cell in the image,

before testing whether each unit cell's adatom sites lie above or below a certain signal limit. Below the limit the location is identified as a molecule (dark spot) and above as a clean adatom. This analysis results in a three-dimensional matrix—two coordinates specify the unit cell and the third specifies the particular adatom (of 12) within the corresponding unit cell.

Figure 1(c) shows for the STM induced process, the results of our unit cell analysis on the pair of before and after images figures 1(a) and (b). Molecules which remain in their original position are indicated by blue (black) spots, originally filled molecular positions that become empty by red (grey) spots and positions that were empty but acquired a molecule by yellow (white) spots. Figure 1(f) shows the equivalent analysis on the before (d) and after (e) images used to measure thermally induced molecular displacement. The sample temperature of figures 1(a) and (b) was  $33.5 \pm 1^\circ\text{C}$  and for (d) and (e)  $30.5 \pm 1^\circ\text{C}$ . The time lapse between image (a) and (b) was 237 s and between (d) and (e) was 242 s. The only significant difference between these two experiments is the manipulation scan taken between (a) and (b). It is therefore apparent that some of the molecular displacements identified in the STM manipulation experiment are in fact thermally generated. Critically, a rigorous analysis of the STM induced process must therefore compensate for thermally induced desorption and diffusion before calculating the correct probability per electron of inducing a molecular desorption or diffusion displacement.

Before examining the thermally driven behaviour of the chlorobenzene/Si(111)- $7 \times 7$  system we check whether the before and after images are really 'passive'. Typical STM images used in this work were  $600 \text{ \AA} \times 600 \text{ \AA}$  in size with  $\sim 1000$  molecules per image. The computer analysis has a resolution of  $\sim 1$  molecular displacement event in 1000 molecules. This limit of sensitivity and the low number of displacement events that occur at temperatures at or below  $24^\circ\text{C}$  mean it is critical that the images taken before and after are strictly passive. Although we have previously shown that at  $+1 \text{ V}$  the probability per electron of displacement is small [20, 21] there is a considerable electric field,  $\sim 10^9 \text{ V m}^{-1}$ , between the tip and surface which could, in principle, perturb the potential energy barriers to diffusion enough for our new more sensitive analysis to be able to detect. To test this possibility, the tunnelling current for a series of images was varied from 2 to 500 pA and the displacement rate of molecules examined at  $24^\circ\text{C}$ . Figure 2 shows that, within experimental error, there was little or no change in the displacement rate as a function of the tunnelling current. Our before and after images are therefore treated as passive in our analysis.

Figure 3(a) presents the rate of thermally induced molecular displacement (i.e., desorption and diffusion) as a function of the sample temperature. Figure 3(b) shows an Arrhenius plot of this data with a standard Arrhenius fit. The best fit parameters give a pre-exponential factor of  $10^{6.2 \pm 0.3} \text{ s}^{-1}$  and an activation energy of  $580 \pm 20 \text{ meV}$ . The displacement measured here is a mixture of desorption and diffusion events and so the Arrhenius parameters cannot be identified with just one process. However, the dominant process at the lower temperatures is diffusion, so the parameters found in this

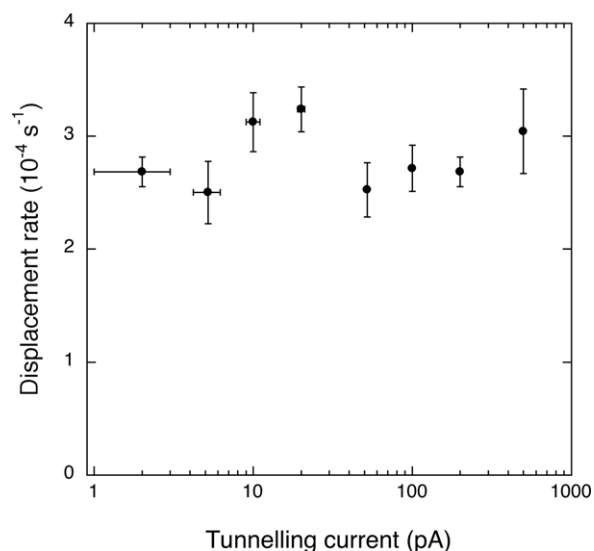


**Figure 2.** Graph to show the minimal tunnelling current dependence of the measured displacement rate at  $+1 \text{ V}$  sample bias and  $24^\circ\text{C}$  (i.e., 'passive' imaging parameters). Each data point is the mean of five pairs of before and after images. Error bars are one standard deviation from the mean of the five experiments. Images were  $600 \text{ \AA} \times 600 \text{ \AA}$  in size and typically contained 1300 molecules. A total of 111 490 molecules were analysed.

regime will reflect mainly this process. Chlorobenzene is known to have a precursor physisorbed state [19, 30, 31] and diffusion will probably proceed via this state. Notably this appears to be reflected in the lower activation barrier found here (580 meV) than that for desorption,  $\sim 1 \text{ eV}$  [20, 30]. Pre-exponential Arrhenius factors are usually taken to be of the order  $10^{13} \text{ s}^{-1}$ , which, in a simple picture, refers to the vibrational 'attempt' frequency to overcome a barrier. Based on the low displacement energy we assume that our measured displacement Arrhenius parameters are dominated by diffusion over desorption. If so, then the low pre-exponential factor of  $\sim 10^6 \text{ s}^{-1}$  reflects the diffusion process more. It therefore suggests that the vibrational modes required for diffusion are soft, for example a rocking mode or ring deformation ( $\sim 40 \text{ meV}$  [30]) which could have momentum parallel to the surface and hence lead to diffusion.

Perhaps the most interesting result of this work is the temperature dependence of the STM induced molecular displacements. Figure 4 presents the probability per injected electron of inducing a molecular displacement both with and without correction for thermally induced displacements. The *uncorrected* probability per electron,  $P_e$ , is calculated from  $P_e = -eL_0^2 \ln(N/N_0)/I_0 t_0 L_m^2$ , where  $e$  is the charge on an electron,  $L_0$  is the size of the manipulation image,  $I_0$  is the tunnelling current,  $t_0$  is the duration time of the STM image,  $L_m$  is the size of one molecule (taken as  $5 \text{ \AA}$ ),  $N_0$  is the number of molecules in the 'before' image and  $N$  the number of molecules that remain in their original positions. To account for thermally induced displacements we correct the molecular populations 'before' and 'after' manipulation. The initial population  $N_0$  is reduced to  $N_0 \exp(-t_0 A \exp\{-E/k_B T\})$  and the final population  $N$  is increased to  $N \exp(t_0 A \exp\{-E/k_B T\})$ . Here  $A$  and  $E$  are



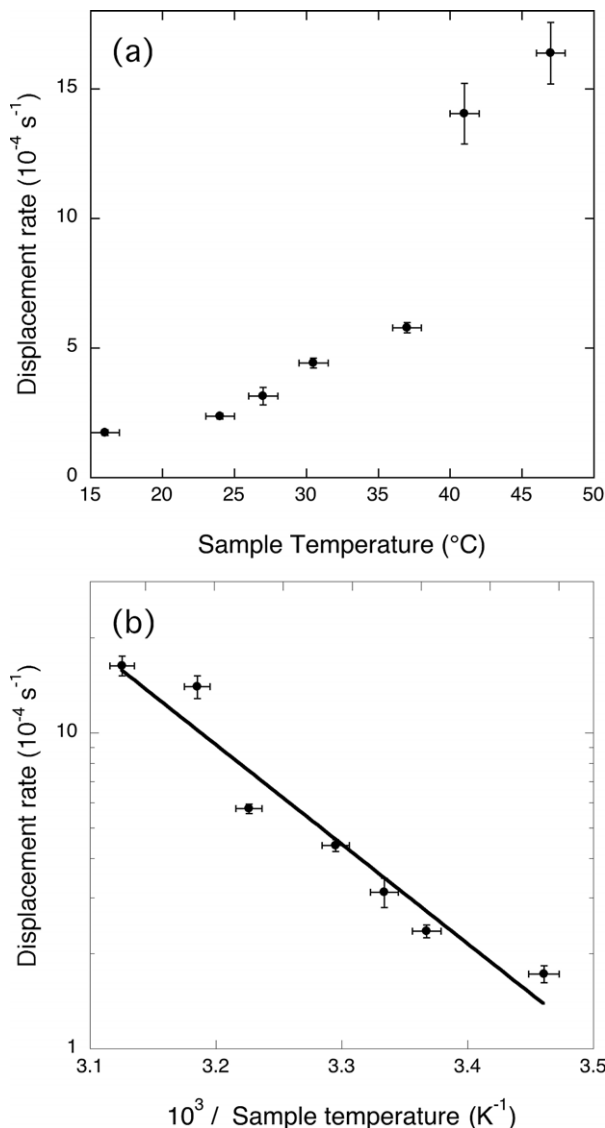


**Figure 3.** (a) Experimental temperature dependence of the rate of purely thermally induced molecular displacement. (b) Arrhenius plot with exponential fit, pre-exponential factor of  $10^{6.2 \pm 0.3} \text{ s}^{-1}$ , activation energy  $580 \pm 20 \text{ meV}$ . Each data point represents an average over 43 pairs of before and after images. Error bars are one standard deviation from the mean. Before and after images were  $600 \text{ \AA} \times 600 \text{ \AA}$  in size. The initial images typically contained 1000 molecules. A total of 550 579 molecules were analysed.

the Arrhenius parameters derived from the fit to the pure thermal displacement data in figure 3(b) and  $t_0$  is the time delay between a molecule being scanned in the ‘before’ image and in the manipulation image. The time delay between a molecule being scanned in the manipulation image and in the ‘after’ image is also  $t_0$ . Whereas in figure 4, the raw data shows a slight decrease in the probability of displacement per tunnelling electron with increasing temperature, the decrease is much more marked in the thermally corrected results.

The underlying reason for this behaviour will be addressed in a future publication. In brief, STM induced displacement is a non-local process where charge injected by the STM tip at a particular surface atomic site is transported across the surface to distant ( $\sim 100 \text{ \AA}$ ) molecules. The calculated probability

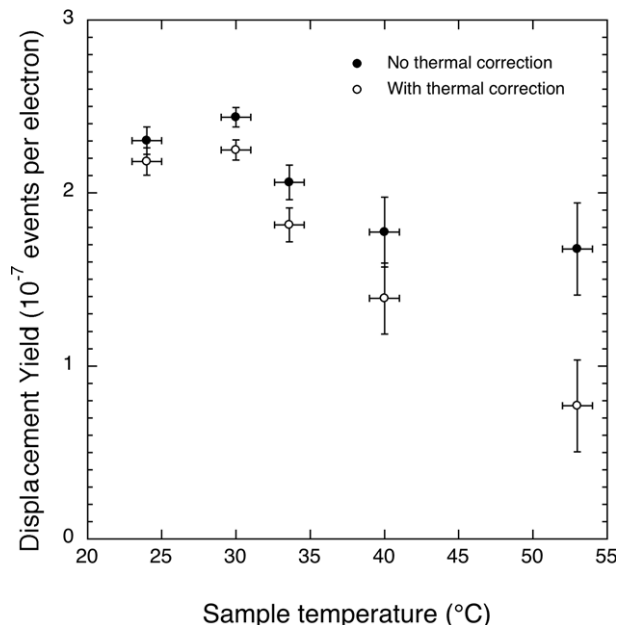


**Figure 4.** Temperature dependence of STM induced molecular displacement, with and without correction for thermally induced displacement. Each data point represents an average over nine before and after images. Error bars are one standard deviation from the mean. Before and after images were  $600 \text{ \AA} \times 600 \text{ \AA}$  in size. The initial images typically contained 700 molecules. A total of 43 712 molecules were analysed.

per electron used in the present work depends linearly on the radial extent of the non-local effect. We therefore conclude that at higher temperatures the decrease in the displacement probability measured here is caused by a reduction of the radial extent in the non-local process. This is probably due to an increase in phonons with a corresponding increase in the probability of electron/phonon scattering of charge away from the surface to the bulk where it cannot initiate displacement of adsorbates.

We have reported the thermal dependence of STM induced molecular displacements (desorption plus diffusion) of chlorobenzene molecules on the Si(111)- $7 \times 7$  surface. Our imaging analysis technique, which compares individual atomic sites in ‘before’ and ‘after’ STM images, compensates for thermal drift and piezo-creep effects. The imaging parameters used before and after a manipulation scan are also shown to be strictly passive. The thermal displacement properties of the chlorobenzene molecules are measured and show Arrhenius behaviour with an activation energy tentatively associated to promotion to a physisorbed molecular state. By this means the thermal behaviour occurring during STM manipulation experiments can be calibrated. Without correction for thermal effects we find a slight decrease in the probability per electron for inducing molecular displacement with increasing temperature, but with thermal correction the reduction is much more marked.

## Acknowledgments

We thank the EPSRC for financial support, SS acknowledges a Thailand Higher Educational Strategic Scholarship.

**References**

- [1] Eigler D M and Schweizer E K 1999 *Nature* **344** 524–6
- [2] Pascual J I, Lorente N, Song Z, Conrad H and Rust H P 2003 *Nature* **423** 525–8
- [3] Stipe B C, Rezaei M A and Ho W 1998 *Science* **279** 1907–9
- [4] Ohara M, Kim Y and Kawai M 2008 *Phys. Rev. B* **78** 4
- [5] Mayne A J, Dujardin G, Comtet G and Riedel D 2006 *Chem. Rev.* **106** 4355–78
- [6] Avouris P and Walkup R E 1989 *Annu. Rev. Phys. Chem.* **40** 173–206
- [7] Ramsier R D and Yates J T 1991 *Surf. Sci. Rep.* **12** 243–378
- [8] Misewich J A, Heinz T F and News D M 1992 *Phys. Rev. Lett.* **68** 3737–40
- [9] Ageev V N 1994 *Prog. Surf. Sci.* **47** 55–204
- [10] Madey T E 1994 *Surf. Sci.* **299** 824–36
- [11] Madey T E, Yakshinskiy B V, Ageev V N and Johnson R E 1998 *J. Geophys. Res.-Planets* **103** 5873–87
- [12] Yakshinskiy B V and Madey T E 1999 *Nature* **400** 642–4
- [13] Dulub O, Batzill M, Solovev S, Loginova E, Alchagirov A, Madey T E and Diebold U 2007 *Science* **317** 1052–6
- [14] Yakshinskiy B V, Wasielewski R, Loginova E, Hedhili M N and Madey T E 2008 *Surf. Sci.* **602** 3220–4
- [15] Palmer R E and Rous P J 1992 *Rev. Mod. Phys.* **64** 383–440
- [16] Palmer R E 1992 *Prog. Surf. Sci.* **41** 51–108
- [17] Salam G P, Persson M and Palmer R E 1994 *Phys. Rev. B* **49** 10655–62
- [18] Christop L G and Stockdal J A 1968 *J. Chem. Phys.* **48** 1956
- [19] Lu P H, Polanyi J C and Rogers D 1999 *J. Chem. Phys.* **111** 9905–7
- [20] Sloan P A, Hedouin M F G, Palmer R E and Persson M 2003 *Phys. Rev. Lett.* **91** 118301
- [21] Sloan P A and Palmer R E 2005 *J. Phys.: Condens. Matter* **18** 1873–85
- [22] Sloan P A and Palmer R E 2005 *Nano Lett.* **5** 835–9
- [23] Sloan P A and Palmer R E 2005 *Nature* **434** 367–71
- [24] Patitsas S N, Lopinski G P, Hul'ko O, Moffatt D J and Wolkow R A 2000 *Surf. Sci.* **457** L425–31
- [25] Alavi S, Rousseau R, Patitsas S N, Lopinski G P, Wolkow R A and Seideman T 2000 *Phys. Rev. Lett.* **85** 5372–5
- [26] Yoder N L, Guisinger N P, Hersam M C, Jorn R, Kaun C C and Seideman T 2006 *Phys. Rev. Lett.* **97** 187601
- [27] Dressler R, Allan M and Haselbach E 1985 *Chimia* **39** 385–9
- [28] Modelli A 2003 *Phys. Chem. Chem. Phys.* **5** 2923–30
- [29] Lucier A S, Mortensen H, Sun Y and Grutter P 2005 *Phys. Rev. B* **72** 235420
- [30] Cao Y, Deng J F and Xu G Q 2000 *J. Chem. Phys.* **112** 4759–67
- [31] Lu X K, Polanyi J C and Yang J 2006 *Nano Lett.* **6** 809–14